# FEATURE ARTICLE

## The Evolution of Surface Chemistry. A Personal View of Building the Future on Past and Present Accomplishments

**G. A. Somorjai**

*Department of Chemistry and Lawrence Berkeley National Laboratory, University of California, Berkeley, California 94720*

Surface chemistry, like other branches of physical chemistry, historically developed through macrosopic studies. These included measurements of adsorption−desorption equilibria (adsorption isotherms), spreading of monomolecular films, surface dissociation of diatomic molecules, and kinetic studies of desorption, sticking, and catalytic oxidation of CO and $H_2$. Models of surface structures were proposed by Langmuir and Taylor on the bases of experimental findings. Molecular level studies of surface chemistry were delayed as compared to other fields of physical chemistry until the late 1950s as instrumentation to detect properties of the very small number of surface atoms ($10^{15}$ cm$^{-2}$) in the presence of a large number of bulk atoms ($10^{22}$ cm$^{-3}$) were not available. At present we have over 65 techniques (photon, electron, molecule, and ion scattering, and scanning probes) that can investigate composition, atomic and electronic structures, and the dynamics of their motion with ≤1% of a monolayer sensitivity. Key results include: quantitative determinations of surface segregation of constituents that minimize surface free energy, discovery of clean surface reconstruction and adsorbate induced restructuring, and the uniquely high chemical activity of rough surfaces and defects (steps and kinks). In situ molecular studies during surface reaction reveal the need for restructuring of metal surface atoms by a highly mobile strongly adsorbed overlayer to maintain catalytic activity: additives that inhibit mobility on the surface poison chemical reactivity. New techniques permitting molecular surface studies at high pressures and at solid−liquid interfaces greatly accelerated the developments of molecular surface chemistry and permitted in situ studies of complex surface chemical phenomena: catalytic reactions, electrode surface chemistry, and polymer surfaces. As always, further developments of techniques control the rate of progress of molecular surface chemistry.

### The Historical Development of Surface Chemistry

Surface chemistry is an important branch of condensed phase physial chemistry, and its development is intertwined with it. In the historical development of physical chemistry the taking of quantitative data served as the foundation of the discipline (also shared by analytical chemistry). Using this database, the laws of thermodynamics could be formulated and tested. Instrumentation development also became an essential part of physical chemistry that was needed to produce even more accurate data. The focus from thermodynamics shifted to investigations of structure and chemical bonding with the rise of quantum mechanics and it was also greatly aided by the developments of X-ray crystallography and spectroscopic techniques. Studies of reaction kinetics gained great popularity focusing first on macroscopic measurements of rate constants and rate equations. Molecular level investigations of chemical systems became gradually predominant including molecular beam studies of reaction kinetics and spectroscopic identification of reaction intermediates of ever shorter lifetimes.

The seminal contributions of Langmuir to the development of surface chemistry occurred during the first four decades of the last century. They were based on macroscopic studies since techniques for molecular studies of surfaces were lacking. His thermodynamic studies explored adsorption−desorption equilibria,[1,2] (adsorption isotherms) and the heats of adsorption and the spreading of monomolecular films of organic molecules on water. His studies of bonding identified the surface dissociation of diatomic molecules[3−6] ($H_2$, $O_2$, and $N_2$) mostly on tungsten. His kinetic studies included CO and $H_2$ oxidation catalyzed by platinum,[7] the desorption rates of H, O and N from W and Mo[6,8−10] and the sticking probability of $H_2$. Although some of the contemporary scientists argued against his assumptions as being too simplistic (for example, Sir Hugh Taylor rightly believed that the surface is structurally heterogeneous with "active sites' for reactions[11] instead of the uniform surface model used by Langmuir to derive his isotherm), much of our conceptual understanding of classical surface chemistry have come from his quantitative investigations. Nevertheless, many other brilliant physical chemists of that age (Emmett,[12,13] Polanyi,[14−16] Freundlich,[17] Bodenstein,[18−21] Taylor,[11] and Rideal,[22,23] to name a few) have made major contributions.

Molecular level studies of surface chemistry came later as compared to molecular investigations of other fields of physical chemistry−and understandably so. The concentration of surface
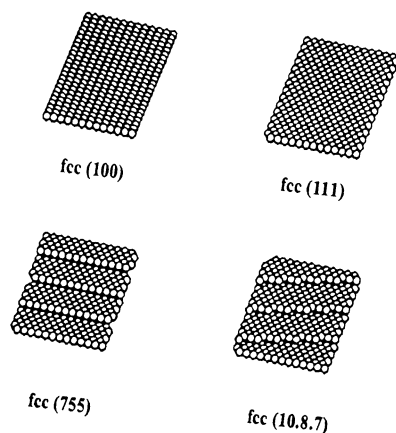
**Figure 1.** Idealized atomic surface structures for the flat Pt(100) and Pt(111), the stepped Pt(755), and the kinked Pt(10, 8, 7) surfaces.

atoms is about $10^{15}$ cm$^{-2}$ while the concentration of atoms in the bulk of a solid or liquid is about $10^{22}$ cm$^{-3}$. As a result one needs techniques for the study of surfaces that are not just surface specific but also highly sensitive to detect the properties of a very small number of atoms in the presence of a large number of bulk atoms. The development of such techniques began in the late 1950s−early 1960s and by now we have over 65 techniques that can investigate surface atoms on the atomic or molecular level with sensitivity of ≤1% of a monolayer to determine composition, atomic, or electronic structures, oxidation states, and also the dynamics of their motion.[24] These are photon, electron, molecule, and ion scattering techniques and scanning probes (scanning tunneling and atomic force microscopies). Since the electron, molecule, and ion scattering techniques were developed first, early studies of molecular surface chemistry were carried out at reduced pressures or at the solid-vacuum interface,[25,26] especially after the invention of high (<10$^{-6}$ Torr) and ultrahigh vacuum (uhv) (<10$^{-9}$ Torr) pumps. The clean solid surface such as one face of a single crystal, obtained and kept in uhv is the simplest type of interface that can be studied by experiment and theory and data obtained on these clean surfaces and their chemical behavior in low-pressure gases that adsorb laid the foundation of quantitative modern surface chemistry.

Most natural surface phenomena, however, occur in the more common chemical environments of atmospheric or higher pressure or at the solid−liquid interface.[27−31] Technological applications of surfaces also utilize these ambients. Over the last 10 years there have been rapid development of techniques (photon scattering and scanning probes) that can be used for molecular studies of the "buried" interfaces, solid (liquid)−high-pressure gas or solid−liquid interfaces. While the discussion of these techniques is beyond the scope of this paper we shall review the highlights of their contributions to our understanding of molecular surface chemistry.

There are three types of surfaces found in nature or used in surface chemistry studies and in surface technologies: the first type is composed of flat surfaces such as those of single crystals that may be cut in different orientations to expose a variety of surface structures (Figure 1), or thin films that are deposited by atomic beam epitaxy or other methods.[24] These are called "external surfaces". The microelectronic circuit is fabricated on such a thin wafer of silicon, or protective coatings are employed in this form. Then, there are microporous surface systems. In these materials most of the surface area is inside the micropores. Molecular sieves[32] or the human bone have this type of structure
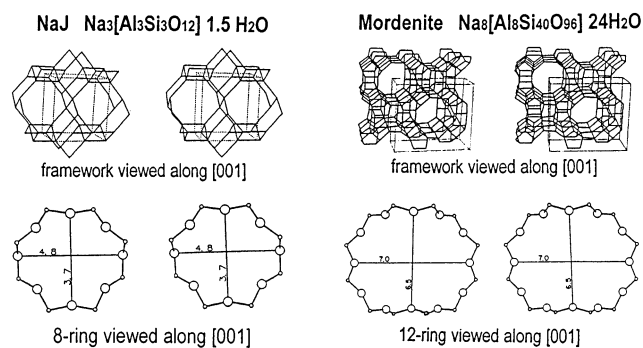


**Figure 2.** Zeolite structure framework for the NaJ (Barrer and White) and mordenite.[32]

(Figure 2). The third type of surface systems are in the form of "nanoclusters". If the cluster is small enough all its atoms are surface atoms (Figure 3). Transition metal catalysts or active sites of many enzymes are in this form. Even for a 1000 atom cluster half of the atoms are surface atoms.

Below we review the frontiers of our understanding of surface properties on the molecular level. We follow the road map of development of physical chemistry in discussing surface chemistry.

## Surface Thermodynamics on the Molecular Scale

**(a) Surface Composition.** Creation of a surface requires energy and thus the free energy of formation of the surface is always positive. To minimize the surface energy the surface area of stable solids or liquids are minimized (solids bound by high atomic density planes and liquids have droplet shapes).[24] In addition there is natural accumulation of atoms or molecules on surfaces that lower the surface free energy. That is why impurities such as carbon or sulfur accumulate on the surface by diffusion from the bulk. For multicomponent systems the surface is always richer in the component that minimizes the surface free energy (surface segregation) (Figure 4) that makes the surface composition always different from the composition in the bulk.[24] At polymer−water interfaces the hydrophilic groups segregate to the surface because water is hydrophilic while hydrophobic groups come to the surface in equilibrium at the polymer−air interface.[33]

**(b) Molecular Adsorption Isotherm.** The concentration of atoms or molecules adsorbed on surfaces depends on their concentration in the gas or liquid above the surface and this relationship is called the adsorption isotherm. Langmuir assumed that all of the surface adsorption sites provide the same binding energy for the adsorbates (uniform heat of adsorption) and this binding energy is independent of the concentration of adsorbates. Molecular surface chemistry studies indicate that the surface is heterogeneous with different sites having different binding energies for adsorbates. In addition the heat of adsorption depends on coverage of adsorbates and it usually declines with increasing coverage due to repulsive adsorbate−adsorbate interactions. Using STM, the adsorption isotherm, the presence of ordering in two dimensions and the coexistence of two or more molecules can be monitored (molecular phase diagram). For example, two ordered phases of NO were found to coexist on the rhodium(111) crystal face in equilibrium with the gas (Figure 5).[34] Their interconversion can be monitored as a function of NO pressure or temperature and their heats of formation and transformation can be measured. There are many

Feature Article

*J. Phys. Chem. B, Vol. 106, No. 36, 2002* **9203**
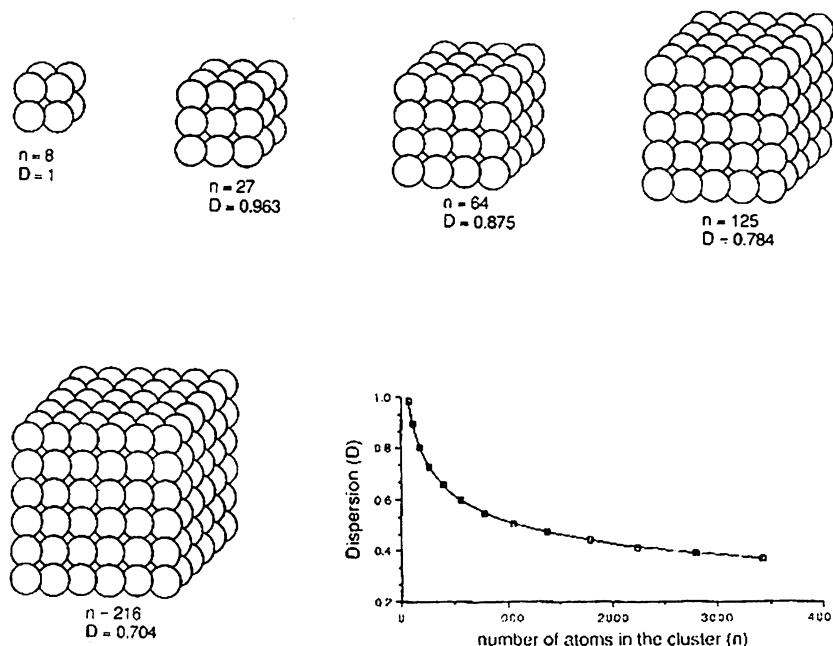


**Figure 3.** Clusters of atoms with single cubic packing having 8, 27, 64, 125, and 216 atoms. In an eight-atom cluster, all of the atoms are on the surface. However, the dispersion, $\mathscr{D}$, defined as the number of surface atoms divided by the total number of atoms in the cluster, declines rapidly with increasing cluster size. This is shown in the lower part of the figure.
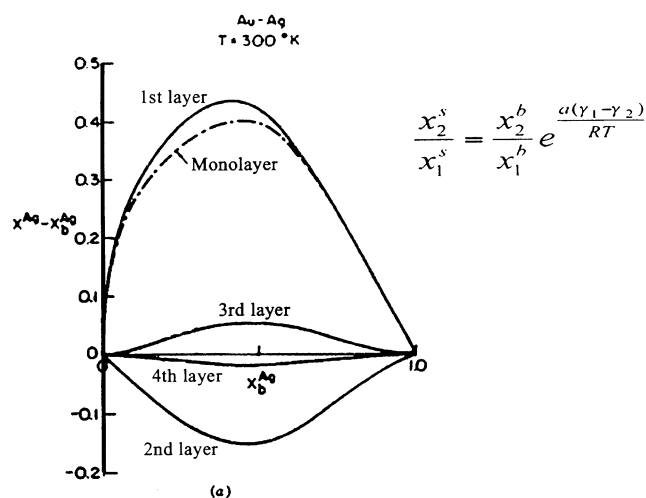


**Figure 4.** Surface segregation in the Au−Ag system. (a) Surface excess of Ag as a function of bulk composition at 300 K.

ordered phases of adsorbed molecules that form in equilibrium with the gas.

**(c) Heat of Adsorption as a Function of Coverage.** Measurements permit quantitative determination of the binding energy of adsorbed molecules at certain surface sites as a function of surface structure and adsorbate coverage. Figure 6 shows the direct measurement of the heat of adsorption of CO by infrared emission as a result of heat evolved during the adsorption on transition metal single-crystal surfaces.[35]

## Studies of Surface Structure and Bonding. Reconstruction and Adsorbate Induced Restructuring

There are many studies on the molecular level of the structure of surfaces and the nature of the surface chemical bond.[24] The workhorse for these studies was low energy electron diffraction surface crystallography,[36,37] which is the X-ray diffraction equivalent for surfaces. Most of these studies were carried out on single-crystal surfaces by measuring the intensities of the diffraction beams as a function of energy. Using a multiple scattering theory the bond distances and bond angles could be obtained from such measurements.[38−40] There are many reasons to expect that the arrangement of atoms at the surface may be different from what it should be if we project the bulk unit cell configuration to a given surface plane. Surface atoms have an anizotropic distribution of neighbors that could yield unsaturated chemical bonds (dangling bonds). Because there are less neighbors than in the bulk their density of electronic states are narrower than for the bulk, approaching that of a few atom containing clusters.[41] Surface crystallography studies showed that the atoms on the surface "relax" inward, which decreases the interlayer spacing between the first and second layer of atoms at the surface as compared to between layers deeper into the bulk. Such a relaxation displaces surface atoms from positions that are optimal for binding to nearest neighbors. To remedy this, clean surfaces often reconstruct; surface atoms rearrange to form unit cells that are very different from what is expected based on the bulk structure. We shall briefly discuss the clean surface reconstruction of four different solids all having different chemical bonding. Figure 7 shows that the (100) surfaces of platinum, gold, and iridium all reconstruct into a hexagonal configuration.[42,43] That is, a hexagonal layer sits on top of the square underlayer that is the projection of the bulk unit cell. This incommensurate lattice structure is the result of changes that occur at the anisotropic interface which realign atoms into a close packed configuration to optimize their bonding. Figure 8 shows the surface structure of ice.[44,45] It was found that the water molecules at the ice surface vibrate with a vibrational amplitude about four times as large as that in bulk ice and this corresponds to the vibrational amplitude of water molecules in water. It appears that the molecules at the top layers of ice are waterlike (disordered) and in many ways they are responsible for the unique properties of ice such as the very low friction coefficient (ice is slippery). Sodium chloride in the bulk, has a structure with alternating sodium cations and chloride

Langmuir

$$\sigma = \frac{\sigma_0 bP}{\sigma_0 + bP} \qquad \Theta = \frac{\sigma}{\sigma_0}$$

**STM (2×2) ⇔ (3×3) NO**

**Phase Diagram**
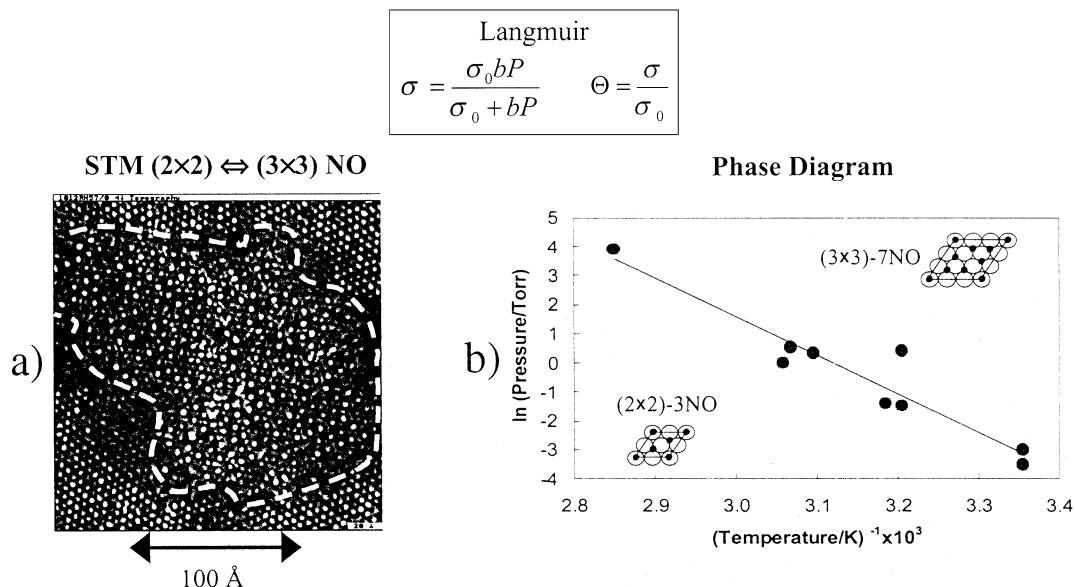
**Figure 5.** (a) A 200 Å x 200 Å STM image taken in 0.03 Torr NO at 25 °C, showing a (3 × 3) domain surrounded by the (2 × 2) structure. It is known that the (2 × 2)-3NO structure contains one top-site NO molecule and two molecules on hollow sites. (b) Plot of ln(*P*) vs 1/*T* for values where the (2 × 2) to (3 × 3) transition takes place. The line though the experimental points separates regions where the (2 × 2) structure is stable (below) and where the (3 × 3) structure is stable (above). The slope of this line is 1.1 ± 0.2 eV/*k*.
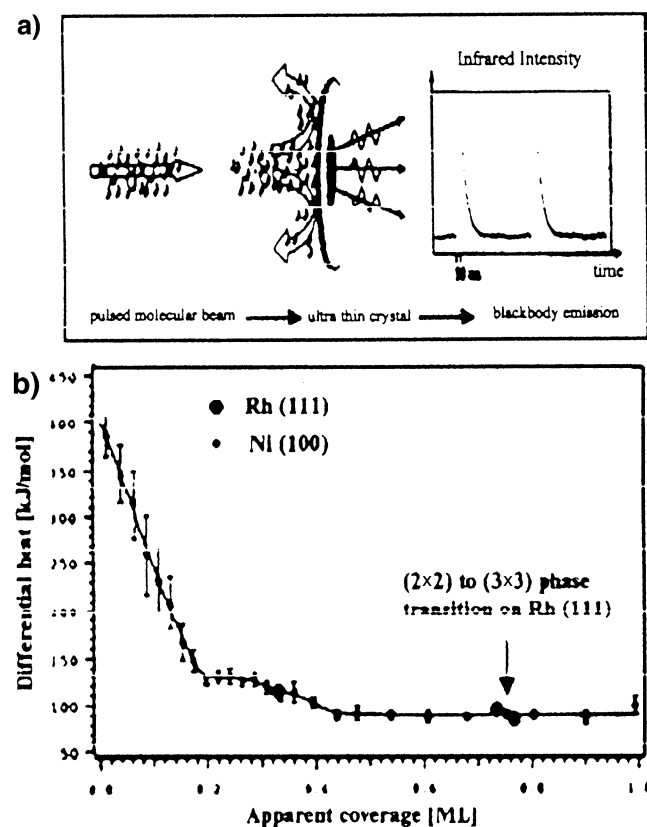


**Figure 6.** (a) Scheme of the experiment for direct measurement of the heat of adsorption of CO in transition metal single-crystal surfaces; (b) heat of CO adsorption as a function of coverage.

anions. At the surface the sodium ions are placed deeper than the chloride ions thereby producing a surface dipole that in fact is the thermodynamically stable surface structure of sodium chloride (Figure 9).[46] All other alkali halides show similar relaxations, and the magnitude of separation of the cation and anion layers at the surface depends on the relative radii of the two ions (for example LiF shows a larger separation than NaCl).

Iron oxide, $Fe_2O_3$, has a bulk structure with alternating iron and oxygen ion layers. At the surface, both oxygen and iron ions are in the same plane. This happens by the large displacement of oxygen ions that moves them into the surface layer.[47]

When adsorbates are placed on clean surfaces additional reconstruction occurs, which is called *adsorbate induced restructuring*.[48] The new chemical bonds that form at the adsorbate substrate interface are optimized by the movement of surface atoms of the substrate to new equilibrium positions. Figure 10 shows an STM study of this phenomenon.[49] The platinum (110) face has one type of structure in the presence of high pressure of hydrogen which is called missing row reconstruction. It has a different structure in the presence of adsorbed oxygen, and again a different structure in the presence of adsorbed carbon monoxide. Because of the difference in the nature of the chemical bonds of the different adsorbates the surface restructures to minimize its energy in different ways, and the surface restructuring shows the optimal surface structure that forms in the presence of a given adsorbate that forms the strongest chemical bonds. In a more quantitative way such a reconstruction can be seen by sulfur adsorption on the rhenium (0001) surface.[50] In Figure 11 the colors indicate the movement of rhenium atoms away from their equilibrium positions in the presence of a monolayer of adsorbed sulfur atoms. The blue atoms are the ones that are in their bulklike equilibrium sites. All the other colors indicate relocation of metal atoms induced by sulfur adsorption. Since the heat of adsorption changes with both the location of the adsorbed atom or molecule on the surface and also with the coverage of the adsorbate, adsorbates induce different types of reconstructions as the structure of the substrate material is altered and also as the coverage of the adsorbate species change.

The restructuring of a metal surface induced by the adsorption of a molecule can be demonstrated by ethylene chemisorption on the platinum(111) and rhodium(111) crystal planes.[51,52] On both metal surfaces the molecule adsorbs on a 3-fold site at 300K with a loss of one hydrogen atom, in the form of ethylidyne, $-C-CH_3$, with its C−C bond perpendicular to the metal surfaces. On the platinum surface it is located on a face centered cubic (fcc) site where there is no metal atom in the

Feature Article

*J. Phys. Chem. B, Vol. 106, No. 36, 2002* **9205**
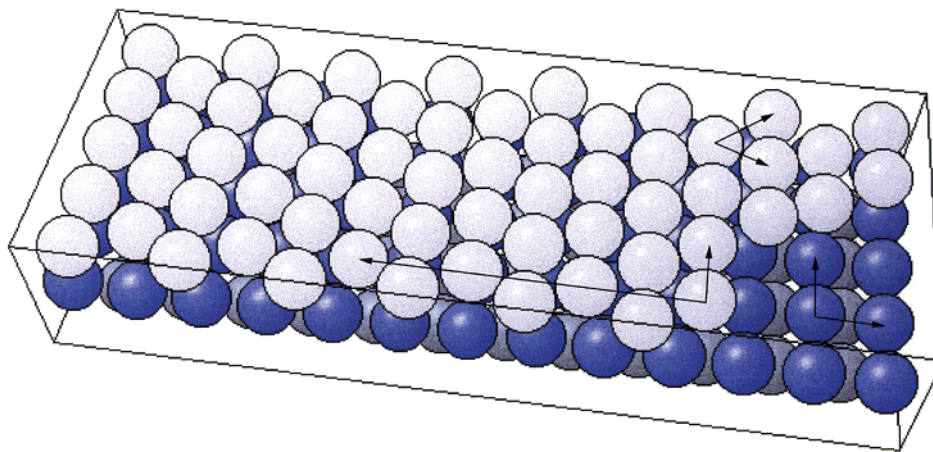


**The reconstructed platinum, gold and iridium (100) crystal faces**

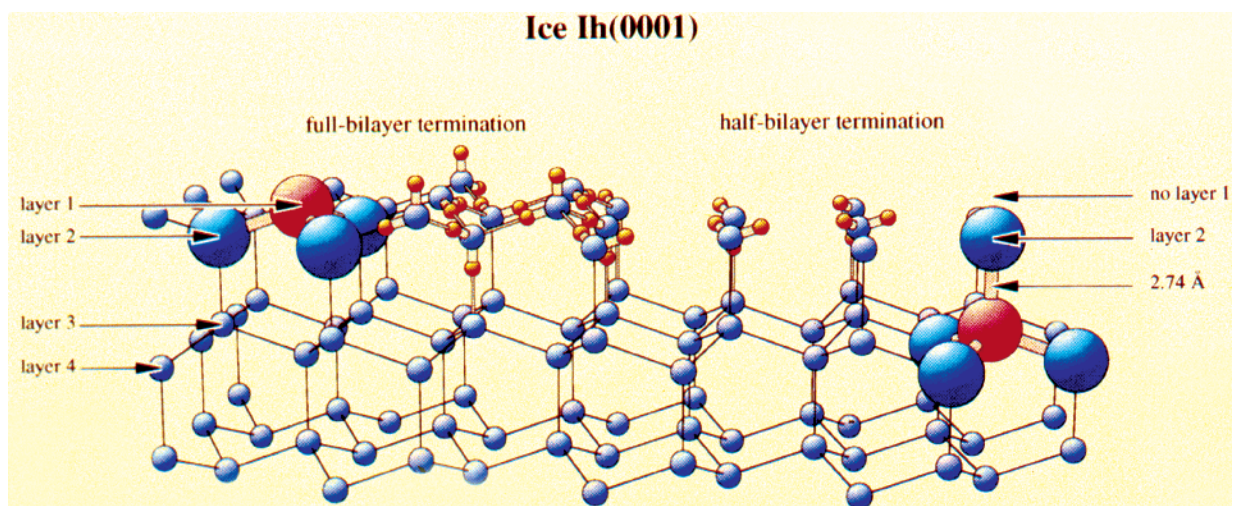**Figure 7.** The reconstructed platinum, gold, and iridium (100) crystal faces.



**Figure 8.** Perspective grazing view of the ice Ih (0001) surface, showing two ideal terminations on top: full-bilayer termination at left (layer 1 is present) and half-bilayer termination at right (layer 1 is absent). Molecules in layer 1 are found to have enhanced vibrational amplitudes, making them invisible in LEED. Middle-size atoms are oxygens, with some hydrogens included as small atoms with assumed bulklike positions and randomness to form $H_2O$ molecules (covalent bonds are drawn medium thick and hydrogen bonds medium thin). Large spheres represent complete $H_2O$ molecules, emphasizing their tetrahedral bulklike bonding arrangement.

second layer directly under the bonding carbon atom. On rhodium it is located on a hexagonal close packed (hcp) 3-fold site where there is a metal atom in the second layer directly under the bonding carbon atom. As seen in Figure 12, the restructuring of the metal atoms around the adsorption sites are quite different. Restructuring occurs to optimize bonding and the energy needed for such a process has two contributions: the heat of adsorption of the molecule which is always exothermic and the rearrangements of the metal−metal bonds that is an endothermic process as it weakens bonding between the metal atoms. The energy balance that also optimizes the adsorbate bond determines the equilibrium surface structure of the adsorbate.
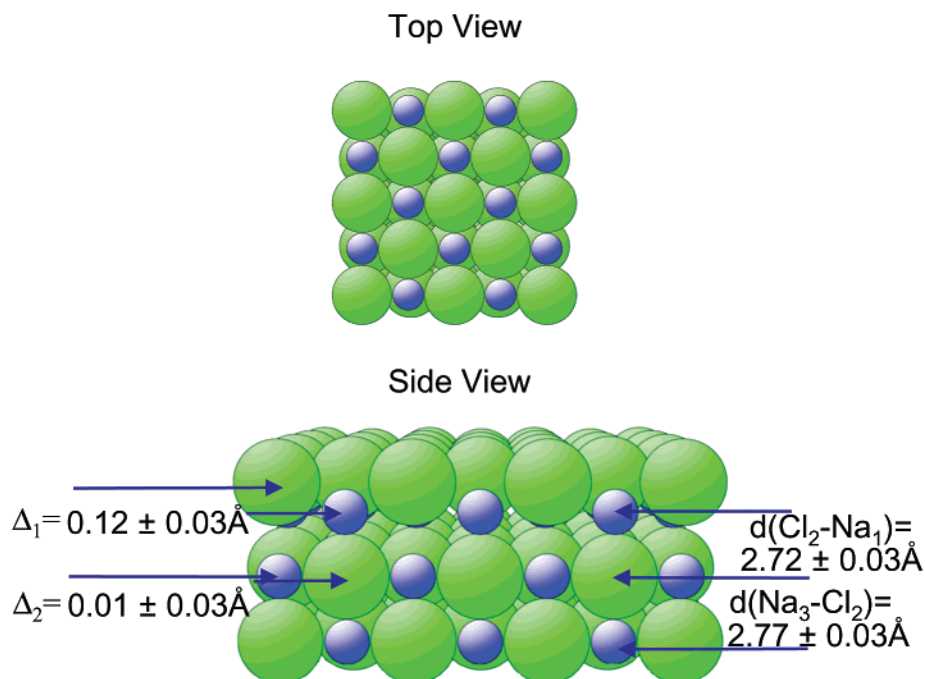
Such studies showed that the nature of the surface chemical bond is clusterlike. The vibrational spectra and the molecular structures of adsorbed molecules on metals are very similar to the spectra and the structure of multinuclear organometallic compounds.[53] In these compounds the metal−metal bond distances are shorter than in the bulk metals. The ability to restructure allows the shortening of metal−metal bonds in the surface, and the adsorbed molecules then tend to form clusterlike

structures, which well-describes the nature of their surface chemical bonds.
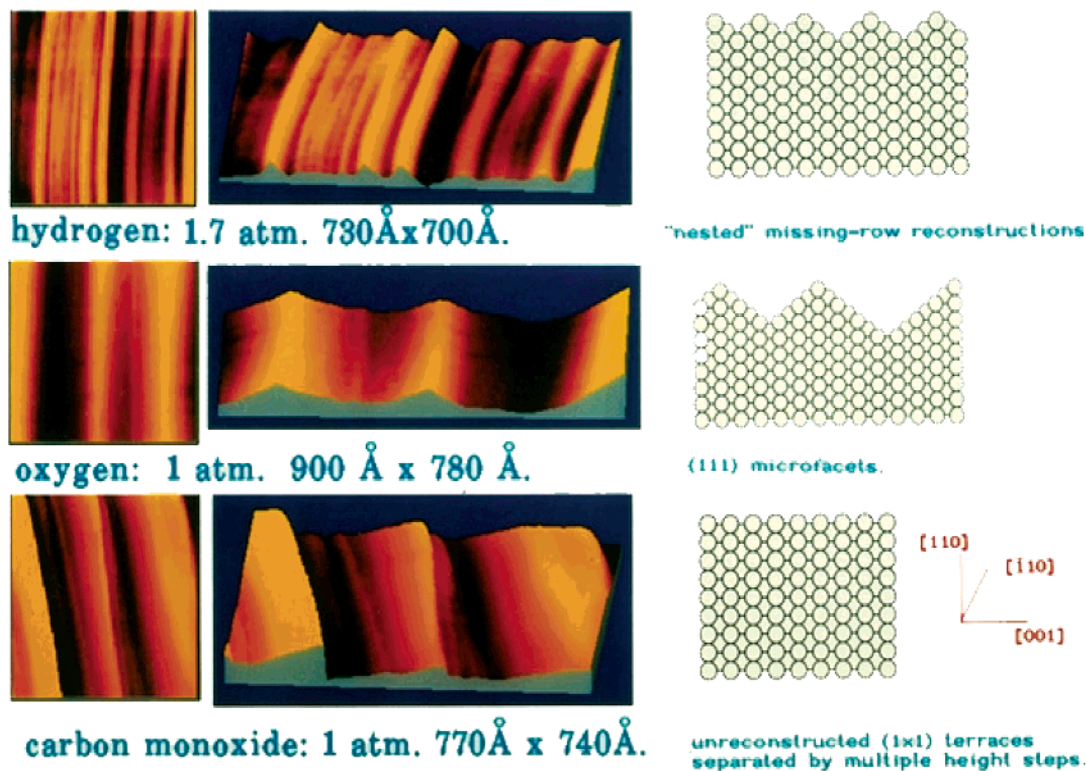
**Rough Surfaces do Chemistry**

Lower coordination surfaces and surface sites that are surrounded by smaller number of nearest neighbor atoms reconstruct more easily. This phenomenon underlies one of the most important findings of surface chemistry; the uniquely high chemical activity of defects at the surface: steps and kinks.[54−68] It has been found that the surface defects are the primary sites where bond-breaking occurs. $H_2\backslash D_2$ exchange occurs at these sites on a platinum surface with unit reaction probability, while on a defect free, step free platinum (111) surface the reaction probability for breaking an H−H bond, which occurs during $H_2\backslash D_2$ exchange is below the detection limit.[56] Experiments reported that C−H,[57−59,61,62,65] C−C,[60,63,64,66] and C≡O[67,68] bond breaking occurs preferentially at defect sites on transition metal surfaces.

The picture of surface structure and bonding that emerges from these studies is one of flexibility.[69−73] The flexible surface restructures as a result of demands of surface chemistry,

## Top View

## Side View

$\Delta_1 = 0.12 \pm 0.03\text{Å}$

$\Delta_2 = 0.01 \pm 0.03\text{Å}$

$d(Cl_2\text{-}Na_1) = 2.72 \pm 0.03\text{Å}$

$d(Na_3\text{-}Cl_2) = 2.77 \pm 0.03\text{Å}$

**Figure 9.** Top view (at left) and side view (at right) of the optimized NaCl (100) surface grown on Pd (100) and Pt (111) (the surface termination is on top); the ionic radii were drawn reduced by 20% for clarity. The values of the interlayer and intralayer spacings in the refined region are shown. The bulk spacings are $\Delta_1 = \Delta_2 = 0.00$ Å and $d(Cl_2 - Na_1) = d(Na_3 - Cl_2) = 2.82$ Å.

## *In Situ* High Pressure STM
### Adsorbate-induced surface reconstructions
### Pt(110) under atmospheric pressures

hydrogen: 1.7 atm. 730Åx700Å.

"nested" missing-row reconstructions

oxygen: 1 atm. 900 Å x 780 Å.

(111) microfacets.

carbon monoxide: 1 atm. 770Å x 740Å.

[110]

[ī10]

[001]

unreconstructed (1x1) terraces separated by multiple height steps.

**Figure 10.** (a) Topographic image of the Pt(110) surface in 1.6 atm of hydrogen after heating to 425 K for 5 h, showing ($n \times 1$) missing-row reconstructions randomly nested. Image size: 730 Å × 700 Å, vertical range $\Delta z = 10$ Å. (b) Topographic image of the Pt(110) surface in 1 atm of oxygen after heating to 425 K for 5 h. Image size: 900 Å × 780 Å, $\Delta z = 25$ Å. (c) Topographic image of the Pt(110) surface in 1 atm of carbon monoxide after heating to 425 K for 4 h. Image size: 770 Å × 740 Å, $\Delta z = 42$ Å. Atomic models of the vertical profile as determined by measurement of lattice spacings and corrugation amplitudes of the reconstruction.

Feature Article

*J. Phys. Chem. B, Vol. 106, No. 36, 2002* **9207**
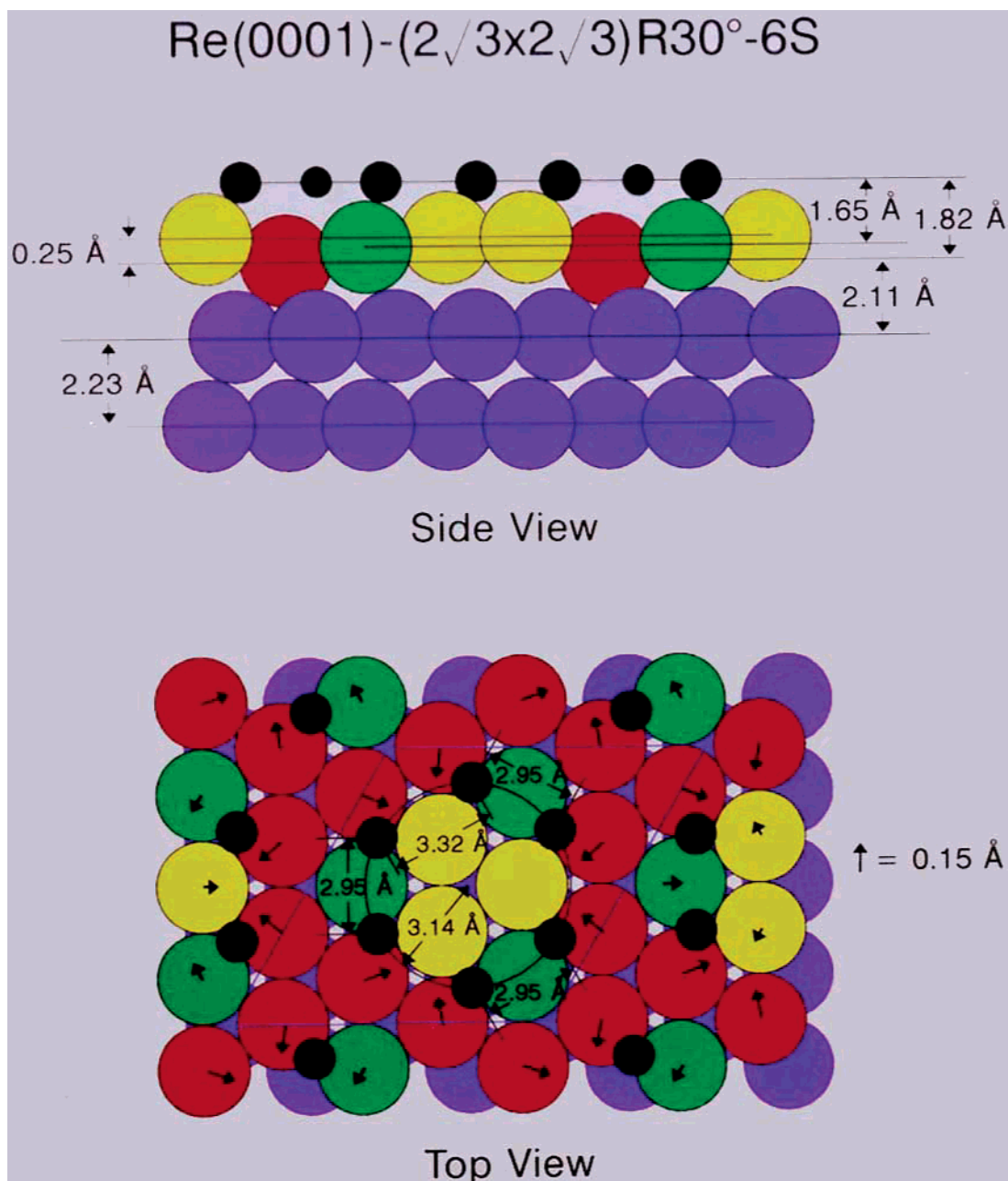


**Figure 11.** Top and side view of the Re(0001)-(2 $\sqrt{3}$ × $\sqrt{3}$) R30°-6S structure. The S sizes (black circles) have been reduced for purpose of clarity. The same shading has been assigned to rhenium atoms equivalent under *p3m1* symmetry in the topmost metal layer. The bulk interlayer spacing is 2.23 Å.

adsorption or chemical reactions. The restructuring gives rise to clusterlike bonding of surface species, and this restructuring appears to be very much enhanced at rough surfaces or at defects, which are sites of low coordination. A simple explanation of this phenomenon brings into focus the balance between the exothermic adsorption process, giving rise to the heat of adsorption, and the endothermic process that weakens metal−metal bonds to restructure the metal in response to adsorption and the formation of the adsorbate−substrate chemical bond. The balance between the exothermic heat of adsorption and the endothermic metal−metal bond weakening gives rise to the final, stable surface structure. Since at defect sites the number of metal−metal bonds is appreciably smaller than in a flat high atomic density metal surface there are less metal atoms to move, and their change of bonding while being weakened, is not as much in need of energy as in a flat surface. As a result the

restructuring of steps- and kink-sites is facile. It appears that bond-breaking chemistry is frequently associated with restructuring of the surface.

It should be noted that the metal clusters in enzymes also show similar restructuring as adsorption and reactions occur. The hydrogenase enzyme that exhibits large changes in the iron−iron distances if hydrogen is present or absent at the active site.[74] Figure 13 shows the nitrogenase enzyme's active site which again undergoes large changes in the iron−iron bond distance as the nitrogen molecule is present or absent at the active site.[75] Living organisms accumulate energy from their environment (in the form of light or redox processes) and store it as conformational change which is used in biosynthetic reactions.[76] Thus substrate (reactant) induced restructuring of active sites and nearest neighbors occur in both biological processes and surface chemistry.
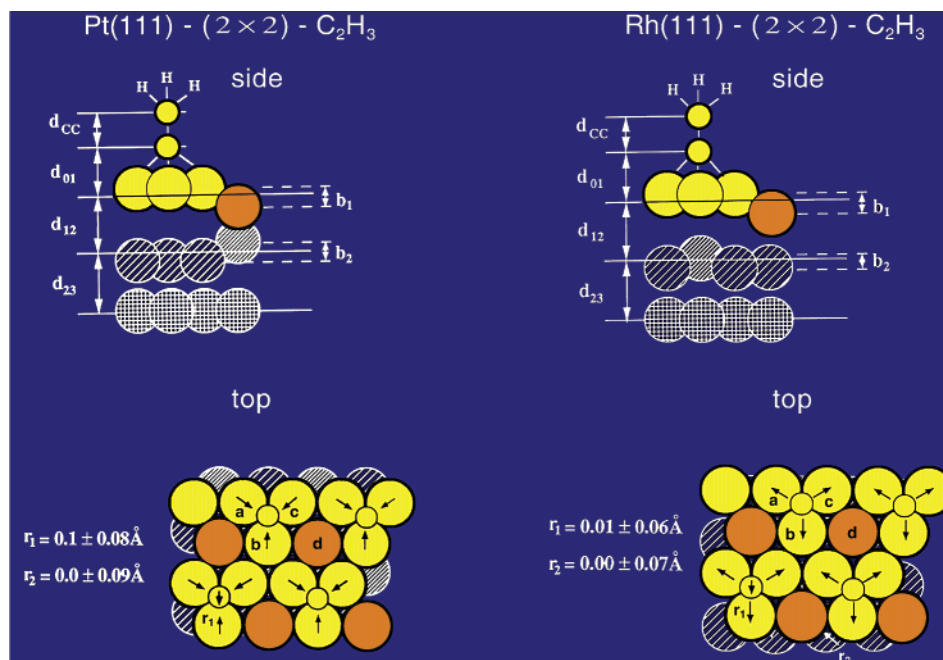
**Figure 12.** Side view of the best-fit, symmetry-preserving, fcc hollow-site model in p(2 × 2) periodicity for CCH$_3$ on Pt(111) with a coverage of 0.25 ML, compared with a model of clean Pt(111) at left. Shading distinguishes the two types of atoms in each substrate layer due to buckling in the ethylidyne model. The buckling is exaggerated in the graph. The distance between the lower carbon and the first metal layer ($d_{01}$) and interlayer spacings ($d_{12}$ and $d_{23}$) are measured between average perpendicular positions of the planes (solid lines). The total buckling amplitudes within the two layers are represented by $b_1$ and $b_2$, respectively. Top view of the best-fit, symmetry-preserving, p(2 × 2) fcc hollow-site model for ethylidyne on Pt(111), exhibiting a radial contraction ($r_1$) of the metal triangle that makes up the hollow site. Shading as in Figure 4. No rotation in the first layer and no lateral motion in the second layer were detected. The hydrogen positions are omitted. Rh (111) − (2 × 2) − C$_2$H$_3$. Side view (top part) and top view (lower part) of Rh(111) (2 × 2)-C$_2$H$_3$ (ethylidyne, with guessed H positions). Gray atoms have relaxed perpendicular to the surface from bulk positions. Substrate relaxations are drawn to scale, emphasized by arrows and labeled by their magnitudes.
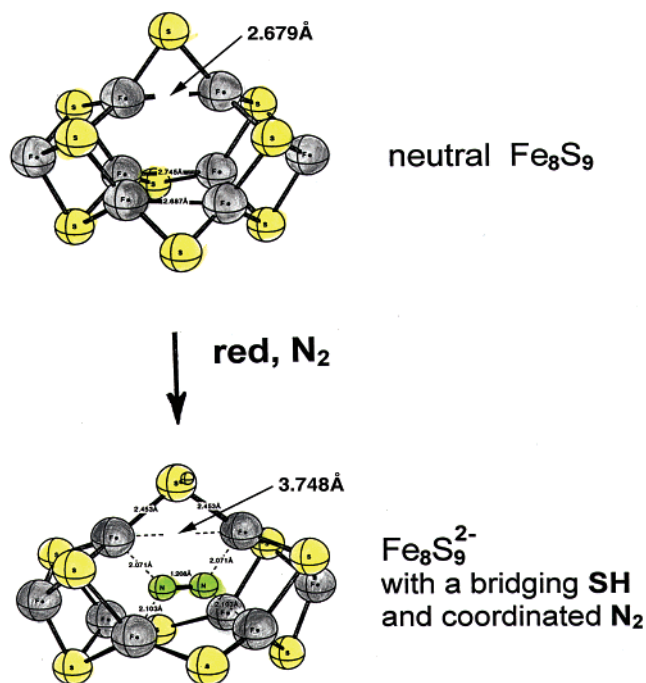


**Figure 13.** N$_2$ activation in FeMo-cofactor of nitrogenase. Note the computed enlargement of the Fe−Fe distance upon N$_2$ adsorption.

Since the surface structure and bonding at surfaces change in different ways during adsorption or surface reactions of each adsorbate and also as a function of coverage, at present molecular surface science studies that can be carried out under reaction conditions at the solid−high-pressure gas and solid−liquid, buried interfaces are at the frontier of research investigations.



$$I(\omega) \propto \left| \chi_{eff}^{(2)} \right|^2 I_1(\omega_1) I_2(\omega_2)$$
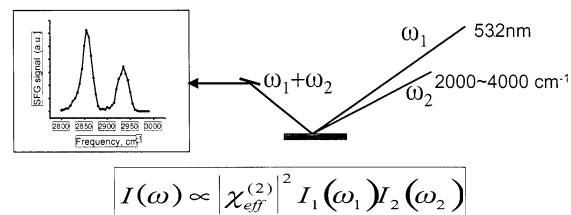
**Figure 14.** Sum frequency generation (SFG) surface specific vibrational spectroscopy. Two laser beams are temporally and spatially overlapped on the surface to generate a third beam at the sum of the two input frequencies. Normally, one input beam is a visible green with a fixed wavelength of 532 nm; the other input beam is tuneable in the infrared region to probe vibrational modes of surface species.

## High-Pressure Surface Science[30]

During the past 10 years new techniques emerged that permit atomic and molecular studies of surfaces at high pressures, in the 1−10$^4$ Torr range. These include scanning probes (atomic force and scanning tunneling microscopies) and optical techniques using lasers or synchrotron radiation. We briefly describe the application of a nonlinear optical technique, sum frequency generation (SFG)−vibrational spectroscopy to the study of surfaces at the solid−high-pressure-gas interface.

Using sum frequency generation (SFG) vibrational spectroscopy, the scheme of which is shown in Figure 14, the spectrum of adsorbed molecules on the surface is detectable over 12 orders of magnitude pressure range.[31,77−79] This is shown in Figure 15. SFG in a nonlinear optical process that must satisfy both the dipole and the polarizability selection rules. Only noncentrosymmetric sites that have no inversion symmetry can do that. As a result the SFG technique is strictly surface monolayer sensitive as compared to infrared spectroscopy that also has signal contributions from the bulk. Another technique, which

Feature Article

*J. Phys. Chem. B, Vol. 106, No. 36, 2002* **9209**
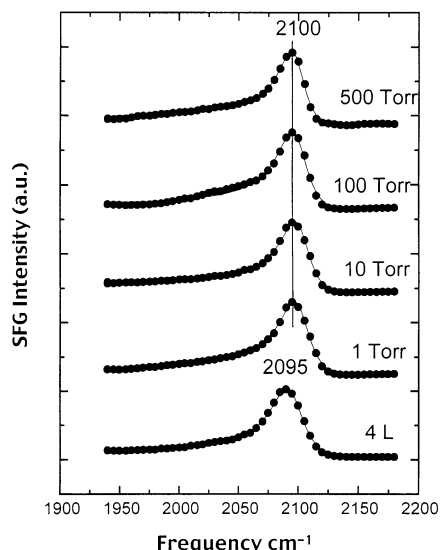


**Figure 15.** SFG spectra of CO on Pt(557) over 12 orders of magnitude of pressure.

is very tolerant to high pressure is scanning tunneling microscopy (STM).[80] A high-pressure cell built around the device permits us to monitor the presence of ordered structures in equilibrium with the gas phase. As a result one can obtain molecular adsorption isotherms that is to detect the structure of adsorbed molecules as a function of coverage which changes with gas pressure as was already discussed in the section on surface thermodynamics. The atomic force microscope (AFM) can also be used over a large pressure range. These techniques serve us well in studies of these buried interfaces on the molecular level.

Perhaps one way to show the tremendous advances that can be made in our understanding of surface chemical processes by in-situ studies is by an example, the hydrogenation of ethylene over platinum single-crystal surfaces.[28] This reaction has a long and important history in surface chemistry and catalysis. Sabatier[81,82] discovered the reaction and Horiuti and Polanyi[16] suggested a mechanism for it in 1934 based on seminal studies that identified $H_2$ dissociation and postulated the formation of the "half-hydrogenated", $C_2H_5$, surface species in an elementary reaction step. SFG studies during catalytic turnover (~12 molecules of ethane produced per platinum site per second) identified three surface species on platinum: ethylidyne, di-$\sigma$-bonded ethylene, and $\pi$-bonded ethylene (Figure 16). The first two molecules are strongly bound to the platinum crystal surfaces ((111) and (100) orientations) and they remain adsorbed on the metal surfaces even after evacuation. The $\pi$-bonded ethylene is weakly adsorbed; it is removed upon evacuation and its surface concentration under steady-state reaction conditions is 4% of a monolayer.[83] Careful surface spectroscopy and reaction rate studies revealed that only the $\pi$-bonded ethylene is a reaction intermediate that hydrogenates rapidly to $C_2H_5$ and then to ethane (Figure 17), the other two strongly adsorbed molecules (ethylidyne and di-$\sigma$-bonded ethylene) are stagnant spectators during the catalytic turnover. Carbon-14 labeling studies verified that ethylidyne remains adsorbed on the platinum surface for over a million turnovers.[61,84] Since the small concentration weakly bound $\pi$-bonded ethylene is the reaction intermediate, the turnover rate per reaction intermediate (which is present in concentrations of only 4% of a monolayer) is 25 times greater than the reported turnover rate per platinum atom. Since $\pi$-bonded ethylene adsorbs on top of a platinum atom (similar to its bonding in
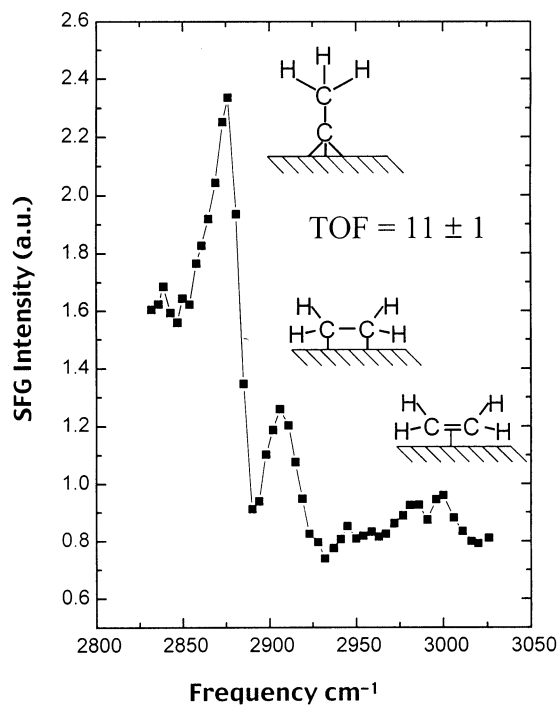


**Figure 16.** SFG spectrum detected during ethylene hydrogenation on Pt(111) with 100 Torr $H_2$ and 35 Torr $C_2H_4$ at 295 K.
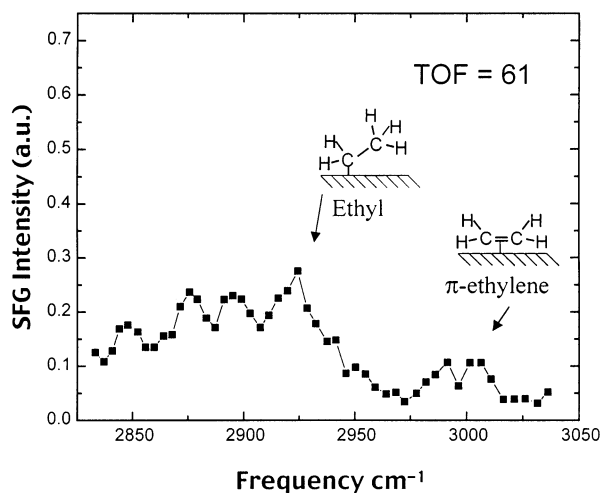


**Figure 17.** SFG spectrum detected for ethylene hydrogenation on Pt(111) at higher $H_2$ pressure of 727 Torr $H_2$ and 60 Torr $C_2H_4$ at 295 K.

organo-metallic molecules) the ethylene hydrogenation reaction is "structure insensitive" since most platinum surfaces have roughly equal number of top sites. The detailed reaction mechanism that can be proposed is shown in Figure 18. When ethylene first adsorbs on the clean platinum surface at the onset of the reaction, it converts to strongly bound ethylidyne or di-$\sigma$-ethylene species that are occupying fcc 3-fold sites and reconstruct the metal surface. Their presence does not prevent the dissociation of $H_2$ as facile $H_2/D_2$ exchange can still be detected. When the surface becomes covered with these species the weakly bound $\pi$-bonded ethylene would adsorb if a proper site is available. This can only occur if some of the ethylidyne molecules diffuse to an hcp hollow site, which would open up a large enough hole in the adsorbed overlayer. STM studies give evidence for disordering of ethylidyne[85] that has an 0.1 eV activation energy of diffusion.[86] The $\pi$-bonded ethylene, once adsorbed, rapidly picks up a hydrogen atom to become $C_2H_5$ half-hydrogenated species (as suggested by Horiuti and Polanyi)
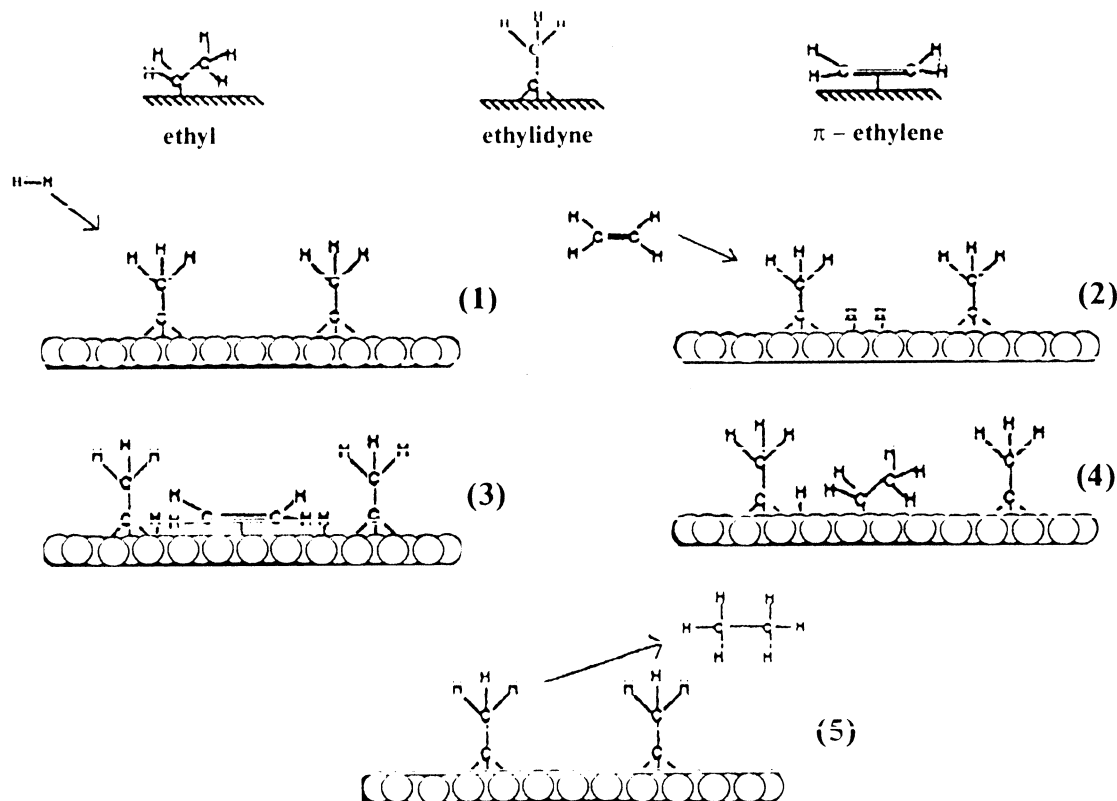
**Figure 18.** Mechanism of ethylene hydrogenation. The strongly adsorbed ethylidyne molecules formed from adsorbed ethylene at first restructure the platinum surface. Their diffusion between fcc and hcp 3-fold sites open up holes on the metal surface that are big enough to adsorb additional ethylene molecules that weakly $\pi$-bond and rapidly hydrogenate to ethyl and then to ethane.

that can be identified in the SFG spectra, which then hydrogenates again to ethane and desorbs.

The important ingredients of catalytic activity of metal surfaces appear to be (1) the restructuring of the metal surface by the strongly adsorbed hydrocarbon overlayer and (2) the mobility of the adsorbed overlayer that makes metal surface sites available for adsorption and reactive turnover of weakly held reactants. Additives that inhibit the diffusion of hydrocarbon species on the metal surface, such as carbon monoxide, will poison the chemical reactivity of the metal.

Since the availability of SFG during high-pressure surface reaction studies the elementary reaction intermediates and reaction steps have been identified for many surface chemical and catalytic processes. These include hydrogenation of propene,[87] 1-butene[88] and cyclohexene,[89] CO dissociation,[90] and oxidation.[91]

### Molecular Studies at Solid Liquid Interfaces

**(a) Surface Chemistry with an External Potential.** The surface electrochemical cell was developed[92] for studies on well-characterized single crystal surfaces. In most investigations of electrochemistry only the transport of electrons have been monitored by measurements of the charge flow in the cell as a function of external potential. With modern surface science techniques one can spectroscopically detect the molecules adsorbed at the electrode-liquid interface that carry the charges or respond to the applied potential in addition to measuring the flow of charges. There are many interesting findings as a result of these studies. For example acetonitrile, $CH_3CN$, as it adsorbs on platinum electrode surfaces, changes molecular orientation as a function of external potential.[93] At low positive potential it forms bonds with the metal surface through its $CH_3$ group

with the CN group away from the surface (Figure 19). At high positive potentials the CN group binds to the metal, and the $CH_3$ group is away from the surface. At potentials in between there is equilibrium between these two differently oriented surface species. A combination of cyclic voltametry and sum frequency generation (SFG)−vibrational spectroscopy was found to be useful to detect changes of molecular structures of adsorbates with changes of external potential.

**(b) Polymer Surface Chemistry.** The human body is full of biopolymer−water interfaces, including the skin, the stomach walls, the brain, the heart, and arteries. An important problem involves the adsorption and structure of proteins at these aqueous interfaces. Bioimplants such as the contact lens or the polymer coated stent that is inserted into arteries become coated with this protein layer, and the lifetime of these implants and the response of the body to them are key areas of research of molecular surface science at the solid−liquid interface.

It was discovered that the polymer surface structure is altered in response to change of the polymer interface from air to water. At the solid−air interface, which appears to be hydrophobic to most polymer molecules, the hydrophobic groups segregate to the surface. At the solid−water interface the hydrophilic groups segregate to the surface of the same polymer after several hours. This is shown for BioSpan polymers, which are polyurethanes with different endgroups.[94] When the endgroups are hydrophobic they are segregated to the surface at the solid−air interface, but when they are placed in water the hydrophilic backbone of the polymer is segregated to the surface (Figure 20). Simultaneously the surface tension changes (as monitored by contact angle measurements) to reflect the changes of surface structure.

In hydrogel contact lenses that contain large concentrations of water in the polymer structure one can monitor the change in surface structure with SFG as the surface dehydrates.[95]
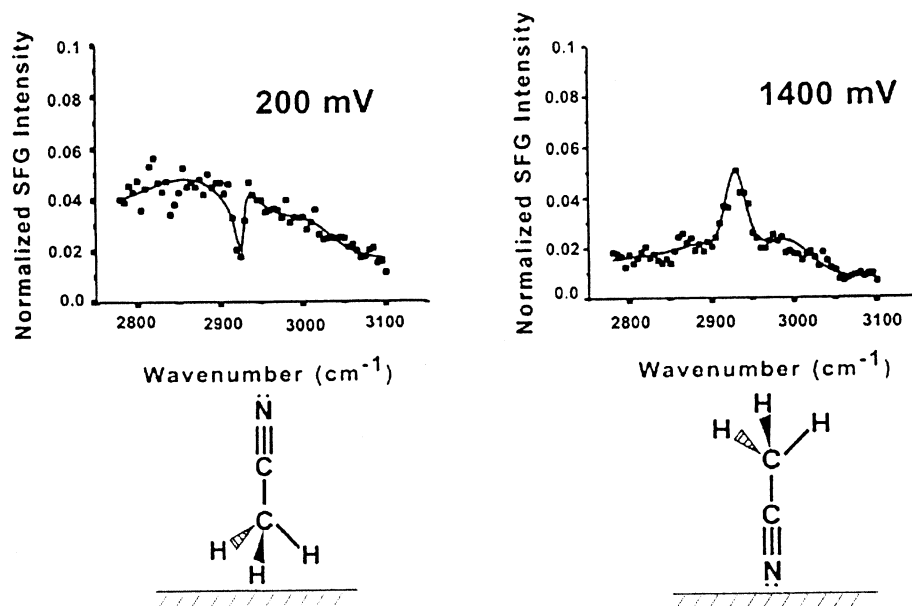
Feature Article

*J. Phys. Chem. B, Vol. 106, No. 36, 2002* **9211**



**Figure 19.** SFG spectra of neat acetonitrile on Pt(111). CH$_3$ up and down orientation.



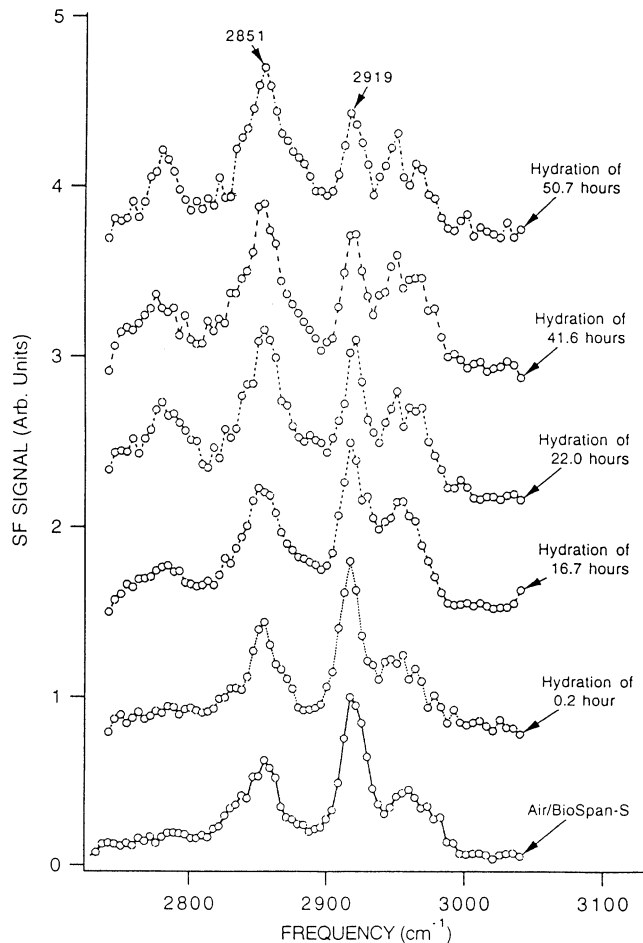**Figure 20.** Time evolution of SFG spectra from the BioSpan-S–water interface. The peak at 2919 cm$^{-1}$ is due to the symmetric stretch of the CH$_3$ group next to the silicone containing hydrophobic end-groups. The peak at 2851 cm$^{-1}$ is due to the symmetric stretch of the CH$_2$ groups that are in the hydrophilic polymer backbone. Note the surface segregation of the hydrophilic groups in water as a function of time.

**Stretching of Polymers is Crucial both in Their Applications in Biological Systems and also as Leather or Rubber Soles and Tires.** The heartbeat gives rise to periodic stretching of the biopolymers in the body that occur frequently (40 million times a year). Atomic force microscopy and SFG are also excellent techniques to study changes of surface structure as the polymer stretches.[96] For example polystyrene–polybutadiene copolymers are rubbers that are frequently used for shoes and rubber bands. In Figure 21 we show the changes in the SFG–surface vibrational spectra and in the friction map obtained by AFM as the rubber is stretched. The soft polybutadiene that has the lower friction coefficient occupies more of the surface than the glassy, more rigid polystyrene as indicated by both SFG and AFM.

**Developments of Techniques Control the Rate of Progress of Molecular Surface Chemistry.** Increased spatial resolution and nanoscale control of surfaces are at the frontiers of instrumentation development. In addition, time resolution of monitoring surface phenomena must be improved to be able to measure dynamics of surface processes on ever shorter time scales. As we move from the millisecond to the femtosecond time scale, new surface phenomena are likely to be discovered with every order of magnitude improvement of time resolution.

## Conclusion

The early decades of the 20th Century provided us with the macroscopic concepts of surface chemistry ranging from the adsorption isotherm to the dissociation of diatomic molecules and their desorption from metal surfaces. Langmuir and his contemporaries were responsible for the lion share of these accomplishments. From the 1960s new techniques permitted atomic and molecular studies of surfaces. The technique developments started in surface physics where applications focused mostly on semiconductor surfaces. During the 25 years that followed, molecular surface studies moved into chemistry. Chemical composition, atomic and molecular structure, surface thermodynamics, and the dynamics of elementary surface reaction steps on the molecular scale were all investigated. New techniques that permitted molecular surface studies at high pressures and at the solid–liquid interfaces greatly accelerated the developments of molecular surface chemistry and permitted in situ studies of more complex surface chemical phenomena; catalytic reactions, electrode surface chemistry and polymer surfaces. Surface chemistry became a molecular science at the
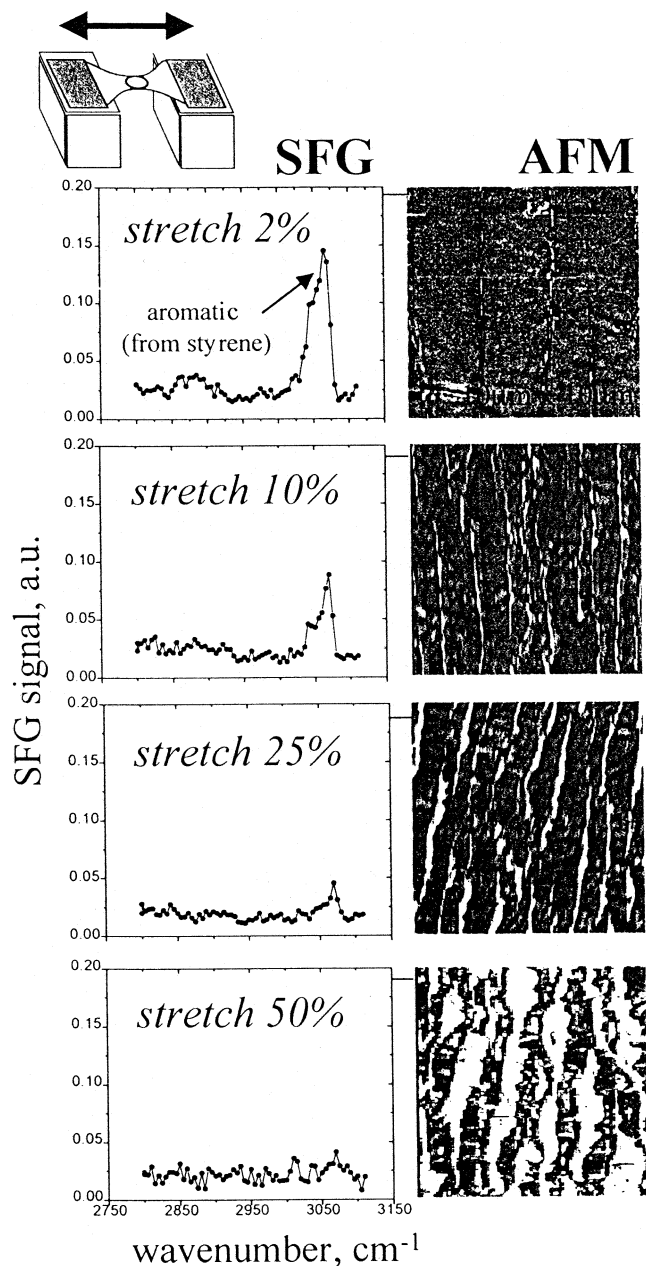
**Figure 21.** SFG spectra and corresponding AFM images of polystyrene−butadiene−styrene) rubber as it is stretched. SFG spectra show that peaks associated with the styrene component decrease on stretching. AFM images show that high friction fracture zones (light regions) are created when the polymer is initially stretched, and expand as the polymer is stretched further. Both techniques indicate that the flexible polybutadiene component segregates to the surface on stretching.

frontier of physical chemistry. These studies provide foundation for surface studies of biological systems. Just as the focus of molecular surface science moved from surface physics to surface chemistry, the next 25 years will see the focus shifting to biology.

**References and Notes**

(1) Langmuir, I. *Phys. Rev.* **1916**, *8*, 149.
(2) Langmuir, I. *Proc. Nat. Acad. Sci.* **1917**, *3*, 141.
(3) Langmuir, I. *J. Am. Chem. Soc.* **1912**, *34*, 860.
(4) Langmuir, I. *J. Am. Chem. Soc.* **1915**, *37*, 417.
(5) Langmuir, I. *J. Am. Chem. Soc.* **1916**, *38*, 1145.
(6) Langmuir, I. *J. Am. Chem. Soc.* **1915**, *37*, 1139.
(7) Langmuir, I. *Trans. Faraday Soc.* **1921**, *17*, 621.
(8) Langmuir, I. *J. Am. Chem. Soc.* **1913**, *35*, 931.
(9) Langmuir, I. *J. Am. Chem. Soc.* **1913**, *35*, 105.
(10) Langmuir, I. *J. Am. Chem. Soc.* **1912**, *34*, 1310.
(11) Taylor, H. S. *Proc. R. Soc. (London)* **1925**, *A108*, 105.
(12) Brunauer, S.; Emmett, P. H.; Teller, E. *J. Am. Chem. Soc.* **1938**, *60*, 9.
(13) Emmett, P. H. *Ind. Eng. Chem.* **1945**, *37*, 639.
(14) Polanyi, M. *Z. Electrochem.* **1920**, *26*, 370.
(15) Polanyi, M. *Z. Electrochem.* **1921**, *27*, 142.
(16) Horiuti, J.; Polanyi, M. *Trans. Faraday Soc.* **1934**, *30*, 1164.
(17) Freundlich, H. *Kapillarchemie*; Leipzig: 1923; Vol. 3. Aufl.
(18) Bodenstein, M. *Z. Phys. Chem.* **1931**, 593.
(19) Bodenstein, M. *Z. Ang. Chem.* **1927**, *40*, 174.
(20) Bodenstein, M. *Z. Electrochem.* **1910**, *16*, 966.
(21) Bodenstein, M. *Z. Electrochem.* **1916**, *22*, 337.
(22) Rideal, E. K. *J. Am. Chem. Soc.* **1920**, *42*, 749.
(23) Rideal, E. K. *J. Chem. Soc. (London)* **1925**, *121*, 1325.
(24) Somorjai, G. A. *Introduction to Surface Chemistry and Catalysis*; John Wiley & Sons: New York, 1994.
(25) Somorjai, G. A. *Annu. Rev. Phys. Chem.* **1968**, *19*, 251.
(26) Blakely, D. W.; Kozak, E. I.; Sexton, B. A.; Somorjai, G. A. *J. Vac. Sci. Technol.* **1979**, *13*, 1091.
(27) McIntyre, B. J.; Salmeron, M. B.; Somorjai, G. A. *Catal. Lett.* **1992**, *14*, 263.
(28) Cremer, P. S.; Su, X.; Shen, Y. R.; Somorjai, G. A. *J. Am. Chem. Soc.* **1996**, *118*, 2942.
(29) Su, X.; Cremer, P. S.; Shen, Y. R.; Somorjai, G. A. *Phys. Rev. Lett.* **1996**, *77*, 3858.
(30) Somorjai, G. A. *Z. Phys. Chem.* **1996**, *197*, 1.
(31) Chen, Z.; Gracias, D. H.; Somorjai, G. A. *Appl. Phys.* **1999**, *B68*, 549.
(32) Meier, W. M.; Olson, D. H.; Baerlocher, C. *Zeolites* **1996**, *17*, 1.
(33) Zhang, D.; Ward, R. S.; Shen, Y. R.; Somorjai, G. A. *J. Phys. Chem.* **1997**, *101*, 9060.
(34) Rider, K. B.; Hwang, K. S.; Salmeron, M.; Somorjai, G. A. *Phys. Rev. Lett.* **2001**, *86*, 4330.
(35) Vattuone, L.; Yeo, Y. Y.; King, D. A. *J. Chem. Phys.* **1996**, *104*, 8096.
(36) Rous, P. J.; Pendry, J. B. *Surf. Sci.* **1989**, *219*, 355.
(37) Rous, P. J.; Pendry, J. B. *Surf. Sci.* **1989**, *219*, 373.
(38) Pendry, J. B.; Heinz, K. *Surf. Sci.* **1990**, *230*, 137.
(39) Pendry, J. B.; Heinz, K.; Oed, W. *Phys. Rev. Lett.* **1988**, *61*, 2953.
(40) Heinz, K.; Oed, W.; Pendry, J. B. *Phys. Rev. B* **1990**, *41*, 10179.
(41) Falicov, L. M.; Somorjai, G. A. *Proc. Natl. Acad. Sci.* **1985**, *82*, 2207.
(42) Van Hove, M. A.; Koestner, R. J.; Stair, P. C.; Biberian, J. P.; Kesmodel, L. L.; Bartos, I.; Somorjai, G. A. *Surf. Sci.* **1981**, *103*, 189.
(43) Van Hove, M. A.; Koestner, R. J.; Stair, P. C.; Biberian, J. P.; Kesmodel, L. L.; Somorjai, G. A. *Surf. Sci.* **1981**, *103*, 218.
(44) Materer, N.; Starke, U.; Barbieri, A.; Van Hove, M. A.; Kroes, G.-J.; Minot, C.; Somorjai, G. A. *J. Phys. Chem.* **1995**, *99*, 7.
(45) Materer, N.; Starke, U.; Barbieri, A.; Van Hove, M. A.; Somorjai, G. A. *Surf. Sci.* **1997**, *381*, 190.
(46) Roberts, J. G.; Hoffer, S.; Van Hove, M. A.; Somorjai, G. A. *Surf. Sci.* **1999**, *437*, 75.
(47) Barbieri, A.; Weiss, W.; Van Hove, M. A.; Somorjai, G. A. *Surf. Sci.* **1994**, *302*, 259.
(48) Somorjai, G. A. *Annu. Rev. Phys. Chem.* **1994**, *45*, 721.
(49) McIntyre, B. J.; Salmeron, M.; Somorjai, G. A. *J. Vac. Sci. Technol. A* **1993**, *11*, 1964.
(50) Barbieri, A.; Jentz, D.; Materer, N.; Held, G.; Dunphy, J.; Ogletree, D. F.; Sautet, P.; Salmeron, M.; Van Hove, M. A.; Somorjai, G. A. *Surf. Sci.* **1994**, *312*, 10.
(51) Starke, U.; Barbieri, A.; Materer, N.; Van Hove, M. A.; Somorjai, G. A. *Surf. Sci.* **1993**, *286*, 1.
(52) Wander, A.; Van Hove, M. A.; Somorjai, G. A. *Phys. Rev. Lett.* **1991**, *67*, 626.
(53) Van Hove, M. A.; Bent, B.; Somorjai, G. A. *J. Phys. Chem.* **1988**, *92*, 973.
(54) Salmeron, M.; Gale, R. J.; Somorjai, G. A. *J. Chem. Phys.* **1977**, *67*, 5324.
(55) Bernasek, S. L.; Somorjai, G. A. *J. Chem. Phys.* **1975**, *62*, 3149.
(56) Salmeron, M.; Gale, R. J.; Somorjai, G. A. *J. Chem. Phys.* **1979**, *70*, 2807.
(57) Somorjai, G. A.; Joyner, R. W.; Lang, B. *Proc. R. Soc. London A* **1972**, *331*, 335.
(58) Blakely, D. W.; Somorjai, G. A. *J. Catal.* **1976**, *42*, 184.

Feature Article

*J. Phys. Chem. B, Vol. 106, No. 36, 2002* **9213**

(59) Herz, R. K.; Gillespie, W. D.; Petersen, E. E.; Somorjai, G. A. *J. Catal.* **1981**, *67*, 371.

(60) Davis, S. M.; Somorjai, G. A. *Platinum Metals Review* **1983**, *27*, 54.

(61) Davis, S. M.; Zaera, F.; Gordon, B. E.; Somorjai, G. A. *J. Catal.* **1985**, *92*, 240.

(62) Zaera, F.; Grodbey, D.; Somorjai, G. A. *J. Catal.* **1986**, *101*, 73.

(63) Gillespie, W. D.; Herz, R. K.; Petersen, E. E.; Somorjai, G. A. *J. Catal.* **1981**, *70*, 147.

(64) Davis, S. M.; Zaera, F.; Somorjai, G. A. *J. Am. Chem. Soc.* **1982**, *104*, 7453.

(65) Davis, S. M.; Somorjai, G. A. *J. Phys. Chem.* **1983**, *87*, 1545.

(66) Davis, S. M.; Zaera, F.; Somorjai, G. A. *J. Catal.* **1984**, *85*, 206.

(67) Iwasawa, Y.; Mason, R.; Textor, M.; Somorjai, G. A. *Chem. Phys. Lett.* **1976**, *44*, 468.

(68) McCrea, K.; Parker, J. S.; Chen, P.; Somorjai, G. A. *Surf. Sci.* **2001**, *494*, 238.

(69) Somorjai, G. A. *Langmuir* **1991**, *7*, 3176.

(70) Somorjai, G. A. *Catal. Lett.* **1992**, *12*, 17.

(71) Somorjai, G. A. *J. Mol. Catal. A.* **1997**, *115*, 389.

(72) Somorjai, G. A. *Theochem.* **1998**, *424*, 101.

(73) Somorjai, G. A. *J. Phys. Chem. B* **2000**, *104*, 2969.

(74) Rees, D. C.; Howard, J. B. *Curr. Opin. Chem. Biol.* **2000**, *4*, 559.

(75) Siegbahn, P. E. M.; Westerberg, J.; Svensson, M.; Crabtree, R. M. *J. Phys. Chem. B* **1998**, *102*, 1615.

(76) Rees, D. C.; Howard, J. B. *J. Mol. Biol.* **1999**, *193*, 343.

(77) Shen, Y. R.; Cremer, P. S.; Su, X.; Somorjai, G. A. *J. Mol. Catal.* **1998**, *131*, 225.

(78) Cremer, P. S.; Su, X.; Chen, Y. R.; Somorjai, G. A. *J. Mol. Catal.* **1998**, *131*, 225.

(79) Su, X.; Shen, Y. R.; Kung, K. Y.; Lahtinen, J.; Somorjai, G. A. *J. Mol. Catal. A* **1999**, *141*, 9.

(80) Jensen, J. A.; Rider, K. B.; Chen, Y. R.; Salmeron, M.; Somorjai, G. A. *J. Vac. Sci. Technol.* **1999**, *17*, 1080.

(81) Sabatier, P. *Ind. Eng. Chem.* **1926**, *18*, 1005.

(82) Sabatier, P. *Die Hydrierung Durch Katalyse*; Academie Verlags-gesellschaft: Leipsig, 1913.

(83) Cremer, P. S.; Su, X.; Shen, Y. R.; Somorjai, G. A. *Catal. Lett.* **1996**, *40*, 143.

(84) Zaera, F.; Somorjai, G. A. *J. Am. Chem. Soc.* **1984**, *106*, 2288.

(85) Erley, W.; Li, Y.; Land, D. P.; Hemminger, J. C. *Surf. Sci.* **1994**, *301*, 177.

(86) Nomikou, Z.; Van Hove, M. A.; Somorjai, G. A. *Langmuir* **1996**, *12*, 1251.

(87) Cremer, P. S.; Su, X.; Shen, Y. R.; Somorjai, G. A. *J. Phys. Chem.* **1996**, *100*, 16302.

(88) Cremer, P. S.; Su, X.; Shen, Y. R.; Somorjai, G. A. *J. Chem. Soc., Faraday Trans.* **1996**, *92*, 4717.

(89) Su, X.; Kung, K.; Lahtinen, J.; Shen, Y. R.; Somorjai, G. A. *Catal. Lett.* **1998**, *54*, 9.

(90) McCrea, K.; Parker, J. S.; P. Chen; Somorjai, G. A. *Surf. Sci.* **2001**, *494*, 238.

(91) McCrea, K. R.; Parker, J. S.; Somorjai, G. A. *J. Phys. Chem.* Submitted for publication.

(92) Baldelli, S.; Ross, P.; Shen, Y. R.; Somorjai, G. A. *J. Phys. Chem. B* **1999**, *103*, 8920.

(93) Baldelli, S.; Mailhot, G.; Ross, P.; Shen, Y. R.; Somorjai, G. A. *J. Phys. Chem.* **2001**, *105*, 654.

(94) Chen, Z.; Ward, R. S.; Y., T.; Baldelli, S.; Opdahl, A.; Shen, Y.-R.; Somorjai, G. A. *J. Am. Chem. Soc.* **2000**, *122*, 10615.

(95) Chen, Q.; Zhang, D.; Somorjai, G. A.; Bertozzi, C. R. *J. Am. Chem. Soc.* **1999**, *121*, 446.

(96) Opdahl, A.; Somorjai, G. A. *J. Polym. Sci., Part B: Polym. Phys.* **2001**, *39*, 2236.